

Experimental and Analytical Study of a Cooling Mechanism Using Acoustic Streaming by Ultrasonic Vibrations

초음파 진동에 의한 음향유동을 활용한 냉각 메카니즘의 실험 및 이론적 연구

Byoung-Gook Loh* and Dong-Ryul Lee †

노병국·이동렬

(2003년 4월 24일 접수 : 2003년 7월 2일 심사완료)

Key Words : Acoustic Streaming(음향유동), Ultrasonic Vibration(초음파 진동), Convective Cooling(대류냉각), Heat Transfer Enhancement(열전달 향상), Resonance(공진)

ABSTRACT

A cooling mechanism using acoustic streaming by ultrasonic vibrations and associated convective heat transfer enhancement is investigated experimentally and analytically. Acoustic streaming pattern and associated heat transfer characteristics are presented. Analytical transient temperature profile of the heated plate following Nyborgs theory is accomplished along with experimental measurement. A temperature drop of 30 °C is obtained in 4 minutes with vibration amplitude of 10 μm . As the vibration amplitude is further increased to 25 μm a temperature drop of 40 °C is achieved that is the maximum temperature drop obtained with the current experimental apparatus. Analytical heat transfer solutions verified a temperature drop of 40 °C with a vibration amplitude of 25 μm at 28.4 kHz which is experimentally obtained.

요 약

초음파 진동에 의한 음향유동을 활용한 냉각 메카니즘과 대류열전달 향상에 관한 연구가 실험 및 이론적으로 수행되었다. 음향유동 형태와 열전달 특성이 제시되었다. Nyborg 이론에 의한 가열판의 이론적 과도 온도분포는 실험에 의해 측정되었다. 10 μm 의 진폭으로 4분안에 30 °C의 온도강하가 발생하였다. 진폭을 25 μm 로 증가시킴에 따라 본 연구의 실험장비에서 습득할 수 있는 최대 온도강하인 40 °C를 얻을 수 있었다. 실험에서 측정할 수 있었던 주파수 28.4 kHz에서의 진폭 25 μm 조건에서의 40 °C의 온도강하를 이론적 열전달 해석으로도 검증할 수 있었다.

1. Introduction

Acoustic streaming produces a quiescent fluid

† Corresponding Author, Member, School of Mechanical and Automotive Engineering, Catholic University of Daegu

E-mail : dlee@cu.ac.kr

Tel : (053) 850-2717, Fax : (053) 850-2710

* Department of Mechanical Systems Engineering, Hansung University

motion near the surface of the object immersed in a high intensity sound field. It is reported that the acoustic streaming is especially effective in promoting certain kinds of rate process occurring on the solid and fluid interface including convective heat transfer, electrical effects, changes in biological cells, and removal of loosely adhering surface layers.⁽¹⁾ A high intensity sound field generated by ultrasonic flexural waves is strong enough to effectively levitate an object above the

beam. Spatial attenuation of a wave in free space and the friction between a medium and a vibrating object⁽²⁾ have been known to generate acoustic streaming. Sound waves are diminished by absorption and scattered as they propagate. This diminution is in general unimportant in a short distance of propagation. However, the propagation of a high intensity sound wave brings about the diminution of pressure significant enough to produce a steady secondary airflow. This type of streaming is usually concerned with a medium of high viscosity. The other type of acoustic streaming results from the fluid shear forces between a medium and a solid surface when the former is oscillating in contact with the latter or vice versa.⁽¹⁾ As long as there is an oscillating tangential relative velocity it is not important whether the source of a relative motion arises from either acoustic oscillations in the fluid or vibrations of the solid. Both cases lead to frictional dissipation within Stokes boundary layer. Unlike acoustic streaming from spatial diminution, this streaming has two components: inner and outer streaming. The inner streaming is created within the boundary layer due to the shear forces between the medium and the wall. Then, the inner streaming also induces relatively large scale steady streaming outside the boundary layer. This process can be compared to the generation of electromagnetic field by a surface current on a conductor.⁽²⁾

The first theoretical analysis of acoustic streaming phenomenon was performed by Rayleigh.⁽³⁾ Further development of the theory was made by Schlichting,⁽⁴⁾ Nyborg,⁽¹⁾ and Lighthill⁽⁵⁾ where emphasis was focused on the fundamental role of dissipation of the acoustic energy in the evolution of the gradients in the momentum flux. In the study of Jackson and Nyborg,⁽⁶⁾ acoustic streaming induced by sonic longitudinal vibration is investigated. Acoustic streaming induced by ultrasonic flexural traveling waves is studied for a

micropump application and negligible heat transfer capability of acoustic streaming is reported.⁽⁷⁾ Gould⁽⁸⁾ investigated heat transfer across a solid-liquid interface in the presence of sonically induced acoustic streaming. Gopinath and Mills^(9,10) investigated convective heat transfer due to acoustic streaming across the ends of a Kundt Tube. Selected references gives an overview of the works done for investigating the heat transfer characteristics of acoustic streaming.⁽¹¹⁻¹³⁾

Therefore, the objective of this paper is to experimentally and analytically investigate the cooling mechanism due to outer acoustic streaming induced by ultrasonic flexural vibrations in an open channel. Primary focus is placed on experimental observation of the cooling phenomenon and comparison with the analytical heat transfer solutions.

2. Theory : Acoustic Streaming

According to the linear acoustics, when sound waves propagate through a medium, the medium itself does not move with the wave but oscillates. This oscillation transmits acoustic energy. However, when a high intensity sound wave propagates, the wave is governed by the nonlinear acoustics and is attenuated by the viscosity and the inertia of the medium, resulting in the pressure gradient along the wave propagation direction. If the gradient is large, the body force is exerted on the medium. As a result, the medium is forced to move with the wave.⁽¹⁴⁾ This phenomenon is known as acoustic streaming. Moroney⁽¹⁵⁾ theoretically explained acoustic streaming based on Nyborg⁽¹⁾ as

$$F = \rho \left[\frac{\partial v}{\partial t} + (v \cdot \nabla)v \right] \\ = -\nabla P + [\mu' + (4/3)\mu] \nabla \nabla \cdot v - \mu \nabla \times \nabla \times v, \quad (1)$$

where F is the body force on the fluid, P is fluid pressure, ρ is density, μ and μ' are shear and bulk viscosity of the fluid, respectively, and v is

particle velocity. It is assumed that P , ρ , and v can be written as a sum of terms of increasing order and decreasing magnitude.

$$\begin{aligned} P - P_o &= P_1 + P_2 + \dots \\ \rho - \rho_o &= \rho_1 + \rho_2 + \dots \\ v &= v_1 + v_2 + \dots \end{aligned} \quad (2)$$

Subscript 0 represents static terms, subscript 1 first order terms, subscript 2 second order terms, etc. The first-order terms, P_1 , ρ_1 , and v_1 are obtained from the linearized Navier-Stokes equations and have a time dependence of $\exp(j\omega t)$, where $j = \sqrt{-1}$, ω is the excitation frequency, and t is time. When interacted with the sound wave in a nonlinear manner, this harmonically varying first-order motion creates a second-order term that consists of a second-harmonic-frequency-doubled term and a zero-frequency term. This zero-frequency term represents a steady fluid flow. The time averaged body force causing the steady flow is estimated from the first-order velocity field as below

$$F \equiv -\rho_o \langle (v_1 \cdot \nabla)v_1 + v_1(\nabla \cdot v_1) \rangle, \quad (3)$$

where $\langle X \rangle$ means "time average of X ". The force in Eq. (3) varies as the square of the first-order

velocity, v_1 , and creates the second-order velocity, v_2 ,

which is calculated from

$$\mu \nabla^2 v_2 - \nabla P_2 + F = 0 \quad (4)$$

The second order velocity, v_2 represents the acoustic streaming velocity and causes circular airflow near an object in a high intensity sound field. Figure 1 shows acoustic streaming near a cylindrical surface vibrating in a typical mode. Normal velocity nodes are at N . The near boundary limiting flow, indicated by heavy solid lines is directed away from nodes of normal velocities. Dashed curves suggest course of return flow. If $v_1 = A \exp(j\omega t)$, where A is the acoustic amplitude, v_2 varies as the square of the acoustic amplitude A which is proportional to the vibration amplitude of the ultrasonic flexural wave.(UFW)

3. Experimental Observations

3.1 Experimental Apparatus

The experimental apparatus shown in Fig. 2 consists of a beam and modules that contain a

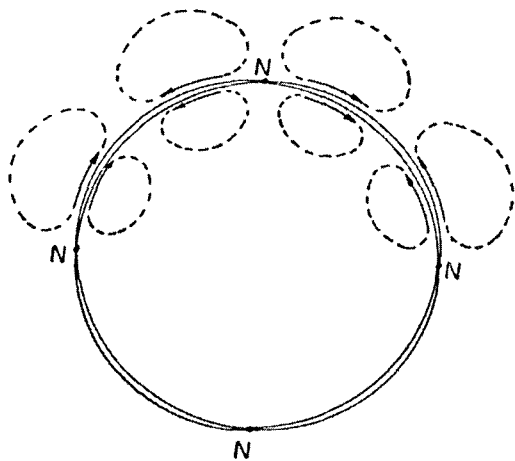


Fig. 1 Acoustic streaming near a cylindrical surface(courtesy of nyborg⁽¹⁾)

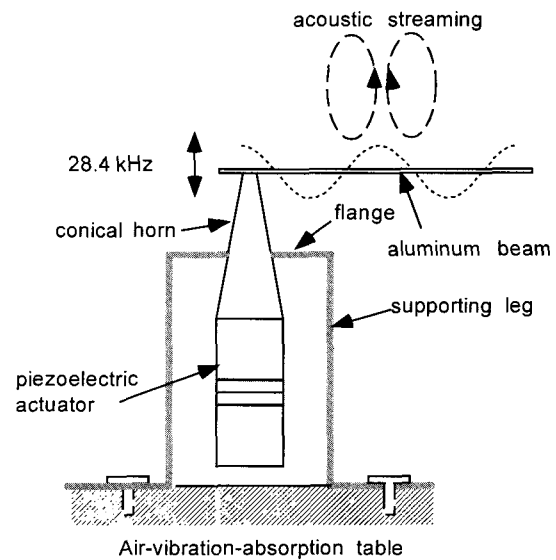


Fig. 2 Experimental apparatus

piezoelectric actuator and a horn. The beam and horn are made of 6061-T6 aluminum due to the excellent acoustical characteristics of this material because aluminum has relatively low damping characteristics. Also, good machining capability of aluminum is one of the reasons to select aluminum as material for the horn and beam.

The piezoelectric actuator is a bolted Langevin type transducer (BLT) designed to resonate at 28 kHz.⁽¹⁶⁾ The conical horn is utilized to increase the amplitude of vibration supplied by the actuator. A conical geometry was selected because it not only gives a desired amplification ratio but also can be easily machined. A mounting flange was included in the design of the horn and is located at the nodal lines where the velocity of vibration of the horn goes to zero. This allowed the mounting of the horn and BLT assembly onto a supporting base plate that was in turn bolted to the surface of an air-driven vibration absorption table. The small end of the horn was threaded to connect the beam with the horn using a machine screw. The dimension of the beam is determined such that one of the natural frequency of the beam is located in the vicinity of the resonant frequency of the actuator, thereby maximizing the displacement of the beam for a given power supply. The determined dimension is 10 mm wide, 1 mm thick and 128 mm long. Frequency spectrum analysis of the system shows that at an excitation frequency of 28.4 kHz, maximum vibration amplitude of the beam is obtained. This frequency is selected as the excitation frequency of the system throughout the experiment because it is found that acoustic streaming velocity is proportional to the vibration amplitude. Therefore, maximum cooling effect of acoustic streaming is most pronounced at the excitation frequency of 28.4 kHz.

3.2 Acoustic Streaming Near the Vibrating Beam

To visualize acoustic streaming near the beam,

the beam is excited at 28.4 kHz with a vibration amplitude of 10 μm . Acetone is sprayed onto the vibrating beam. When Acetone comes in contact with the beam it becomes small droplets and follows airflow pattern near the beam until it completely evaporates.

A fiber optic lamp locally illuminates the region near the vibrating beam. Light is reflected from only Acetone droplets and the beam, making ambient air appear black. The whole process is videotaped using a camcorder. Figure 3 shows a snap shot of the process. Unique features of acoustic streaming are observed. First, air rises above the anti-nodes and descends toward the nodes. Since vibration amplitude is not uniform along the length of the beam, the maximum distance to which Acetone droplets rise above the anti-nodes are not uniform either. Second, there exist two distinctive circular secondary airflow within half wavelength that is 1 cm for this case. Clearer acoustic streaming is observed with bigger vibration amplitude.

3.3 Convective Cooling Mechanism

In order to measure the convective heat transfer enhancement due to acoustic streaming, a heat source containing an aluminum plate, a resistor,

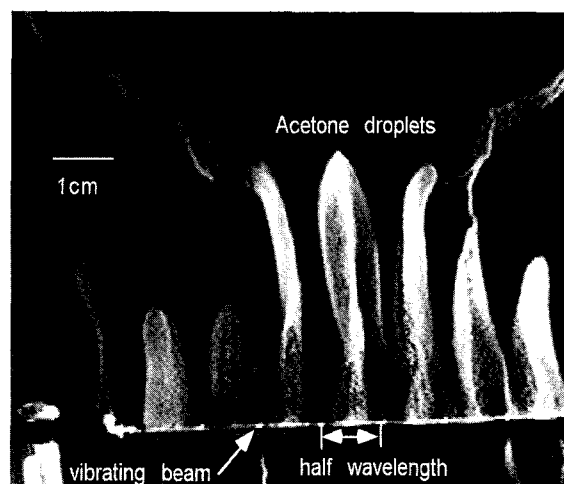


Fig. 3 Visualization of acoustic streaming

and a thermocouple is made. A detailed schematic diagram of the plate is shown in Fig. 4.

The bottom of the plate is made of aluminum. The top is made of Plexiglas that contains a 600Ω resistor and a thermocouple. The resistor is connected to a variable voltage power supply and serves as a heater.

With the 600 Ω resistor, the temperature of the plate can be increased to 98 °C. During the experiment, the room temperature was kept at 20 °C. The heat source is placed 1.5 mm above the vibrating beam. As the temperature of heat source reaches a steady state value of 98 °C with a power supply of 3.4 Watt, acoustic streaming is generated by vibrating the beam at 28.4 kHz with a vibration amplitude of 10 μm. Vibration amplitude is measured using capacitance gauge which has a resolution of 80 nm.

Then, the temperature changes of the plate are measured using the thermocouple (T-type, Omega Eng., Inc.). Due to the inherent noises in the voltage signal from the thermocouple, the signal is filtered through a low pass filter and sampled at 20 Hz using a data acquisition board.

4. Analytic Heat Transfer Solutions

4.1 System Model and Governing Equations

Figure 5 shows schematically the two-

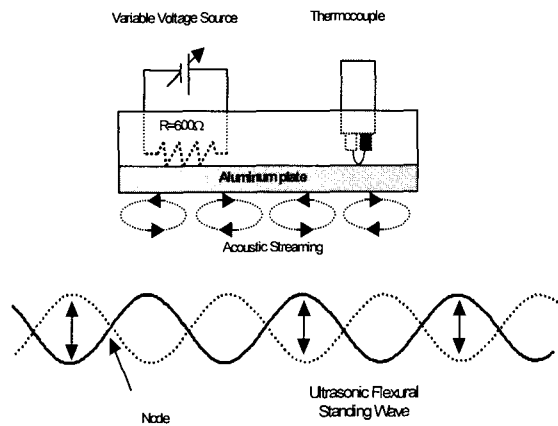


Fig. 4 Schematic diagram of heat source

dimensional channel model of the ultrasonic flexural standing waves (UFSW) system. The model consists of the lower, very thin vibrating plate (UFSW) and the upper rigid three-layer plate with a controlled volumetric heat source. ($\dot{q} = 3.2 W$) The vertical displacement of the lower vibrating plate is given by

$$y = A(t) \cos(2\pi x/\lambda) \quad (5)$$

where $A(t)$ is the wave amplitude, $A(t) = A_0 \sin(\omega t)$. The mathematical models described below are 1-D and 2-D simplifications of the actual experimental apparatus discussed previously.

The Reynolds number based on the representative conditions, i.e., the thickness of the gap is 2 mm, A_0 is 25 μm, λ is 1 cm, and f is 28 kHz, is less than 1800, which is in the region of laminar flow. The air velocity in the gap is less than Mach 0.3 so that the incompressible fluid assumption can be applied. The governing equations for incompressible transient laminar

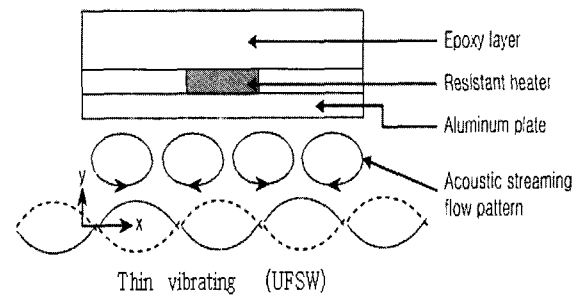


Fig. 5 Schematic diagram of the system

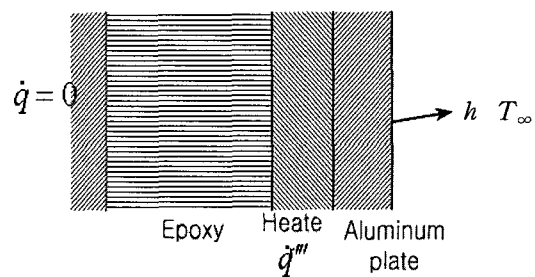


Fig. 6 1-D Analytic heat transfer model

Newtonian fluid flow are continuity equation as follows:

$$\nabla \cdot \bar{\mathbf{v}} = 0 \quad (6)$$

and linear momentum equation:

$$\frac{\partial \bar{\mathbf{v}}}{\partial t} + (\bar{\mathbf{v}} \cdot \nabla) \bar{\mathbf{v}} = \frac{1}{\rho} (-\nabla p + \mu \nabla^2 \bar{\mathbf{v}}) \quad (7)$$

The velocity $\bar{\mathbf{v}}$, which contains harmonic terms and a "dc" term, is calculated from Eq. (6) and (7) and the acoustic streaming velocity ($\bar{v}_{a,i}$, $i = 1, 2, 3$), is obtained by averaging $\bar{\mathbf{v}}$ over a period as follows:

$$\bar{v}_{a,i} = \frac{1}{T_a} \int_0^{T_a} v_i dt \quad i = 1, 2, 3 \quad (8)$$

where T_a is the period. Using the acoustic streaming velocity obtained from Eq. (8), the convective heat transfer equation can be solved numerically, which is given by

$$\rho C_p \frac{DT}{Dt} = k \nabla^2 T + \mu \left(\frac{\partial \bar{v}_{a,i}}{\partial x_j} + \frac{\partial \bar{v}_{a,j}}{\partial x_i} \right) \frac{\partial \bar{v}_{a,i}}{\partial x_j} \quad (9)$$

where i and $j = 1, 2, 3$. The lumped energy approach is applied to the transient 1-D system shown in Fig. 6 with heat generation in the plate and heat loss through the surfaces, i.e.,

$$\frac{dE}{dt} = -2Aq_n \quad (10)$$

where A describes the surface area of one side of the plate and q_n is the heat flux at the surface.

The left hand side of Eq. (10) can be expressed as

$$\frac{dE}{dt} = \rho (2AL) C_p \frac{dT}{dt} - (2AL) \dot{q}''' \quad (11)$$

where L is the plate thickness, C_p is the specific heat of the plate material, T is the lumped

temperature of the plate, and \dot{q}''' is the constant heat generation rate in the plate. Thus, the energy balance for this system can be stated as

$$\rho LC_p \frac{dT}{dt} = -q_n + L\dot{q}''' \quad (12)$$

with the initial and boundary conditions given by

$$T(0) = T_i \quad \text{and} \quad q_n = h(T - T_\infty) \quad (13a,b)$$

where T_∞ is the ambient air temperature outside the thermal boundary layer.

Substituting Eq. (13b) into (12) gives

$$\rho LC_p \frac{dT}{dt} = -h(T - T_\infty) + L\dot{q}''' \quad (14)$$

subject to Eq. (13a). The time-dependent temperature distribution is given by

$$T = \left(T_\infty + \frac{\dot{q}''' L}{h} \right) + \left(T_i - T_\infty - \frac{\dot{q}''' L}{h} \right) \exp \left(-\frac{ht}{\rho C_p L} \right) \quad (15)$$

where T_∞ , \dot{q}''' , and T_i are known and h can be estimated for infinite rectangular tubes.⁽¹⁷⁾

5. Results and Discussion

The temperature of the upper heated plate can be increased to 98 °C with the proposed power supply. During the experiment, the room temperature was maintained at 20 °C. As the temperature of heat source reaches a steady state value of 98 °C, acoustic streaming is induced by vibrating the lower surface at 28.4 kHz with a vibration amplitude of 10 μm. In order to ascertain the convective heat transfer enhancement due to acoustic streaming, the transient temperature of the heat source was measured. A temperature drop of 30 °C is obtained in 4 minutes with vibration amplitude of 10 μm and maintained as shown in Fig. 7. As the vibration amplitude is further increased to 25 μm a temperature drop of

40 °C is achieved that is the maximum temperature drop obtained with the current experimental apparatus.

Figure 8 shows the time-dependent temperature distributions for the upper plate obtained with the analytic solution (Eq. (11)) as well as experimental temperature measurements. The initial temperature of the plate, T_i , and the air temperature, T_∞ , were given as 96.8 °C and 20.0 °C, respectively, and the calculated temperature at time $t = 300$ sec. is compared to the measured temperature

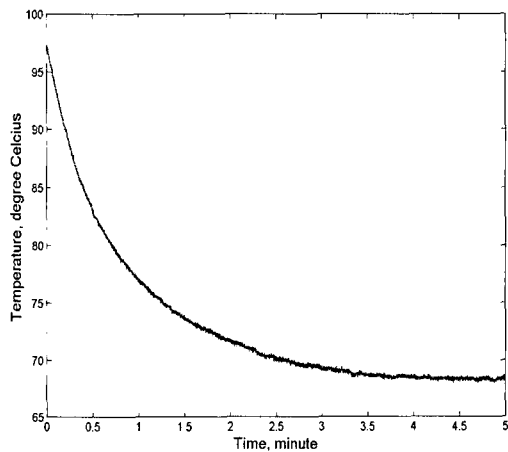


Fig. 7 Transient temperature drop of the heat source

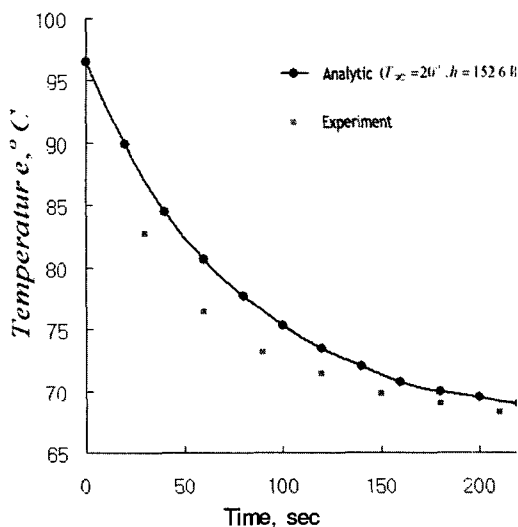


Fig. 8 Transient temperature profile of the heat source(analytic solution and experiment)

($T_{\text{measure}} = 68.0 \text{ }^\circ\text{C}$). From the analytic heat transfer solution, the convective heat transfer coefficient, h , for this system with a 3.2 Watt heat generation rate is calculated as $152.6 \text{ W/m}^2\text{K}$. In comparison, using thermal-entry-length Nusselt number value with the maximum acoustic streaming velocity for the base case, the heat transfer coefficient is about $141.0 \text{ W/m}^2\text{K}$, which is within acceptable bounds.⁽¹⁷⁾ With the constant convective heat transfer coefficient value, $h = 152.6 \text{ W/m}^2\text{K}$, the temperature profile of the upper aluminum plate is obtained using Eq. (11). For this analytical calculation, it is assumed that there is no temperature gradient in the thin aluminum plate, the temperature and the thermal properties are for the thermal insulator or heat generator (material: epoxy), the thickness of the plate is assumed 5 mm, which is the total thickness of the upper plate assembly, and the back side of the upper plate assembly is insulated to maintain the direction of the heat flux toward the surface.

Using the analytic convective heat transfer solutions using Eq. (11) (cf. Fig. 8), the transient temperature profile of the upper aluminum plate is similar to that obtained from experimental measurements.

6. Conclusions

A cooling mechanism using acoustic streaming by ultrasonic vibrations and associated convective heat transfer enhancement are experimentally and analytically investigated. Acoustic streaming pattern and associated heat transfer characteristics are presented. Analytical transient temperature profile of the heated plate following Nyborgs theory is accomplished along with experimental measurement. A temperature drop of 30 °C is obtained in 4 minutes with vibration amplitude of 10 μm . As the vibration amplitude

is further increased to $25\ \mu\text{m}$ a temperature drop of $40\ ^\circ\text{C}$ is achieved that is the maximum temperature drop obtained with the current experimental apparatus. Analytical heat transfer solutions verified a temperature drop of $40\ ^\circ\text{C}$ with a vibration amplitude of $25\ \text{m}$ at $28.4\ \text{kHz}$ which is experimentally achieved.

Using analytical convective heat transfer solutions, the time-dependent temperature drop of the heated plate can be reproduced assuming an effective heat transfer coefficient of $152.6\ \text{W/m}^2\text{K}$. From the analytical heat transfer solutions, it is very important to include a reasonable heat transfer coefficient for the lower plate, which is long and of high conductivity material. Using appropriate boundary conditions, the time-dependent temperature contour fields is obtained and compared to the measured temperature drop for the heated surface. The heat loss from actual three-dimensional flow fields and subsequent heat transfer effects is much larger than the heat loss through the lower surface of the upper plate assembly. Hence, it is recommended that three-dimensional flow field simulations as well as convective heat transfer simulations should be conducted to obtain more realistic solutions without resorting to prescribed effective heat transfer coefficients.

Acknowledgments

This research was financially supported by Hansung University in the year of 2003.

References

- (1) Nyborg, W. L., 1958 Acoustic Streaming Near a Boundary, *J. of Acoust. Soc. Am.*, Vol. 30, No. 4, pp. 329~339.
- (2) Lee, C. P. and Wang, T. G., 1990, "Outer Acoustic Streaming," *J. of Acoust. Soc. Am.*, Vol. 88, No. 5, pp. 2367~2375.
- (3) Rayleigh, 1945, *Theory of Sound*, Dover Publication, New York.
- (4) Schlichting, H., 1955, *Boundary Layer Theory*, McGraw-Hill Book Company, Inc., New York.
- (5) Lighthill, J., 1978, "Acoustic Streaming," *J. of Sound and Vib.*, Vol. 6, No. 3, pp. 391~418.
- (6) Jackson, F. J. and W. L. Nyborg, 1960 "Sonically-induced Microstreaming Near a Plane Boundary. I. The Sonic Generator and Associated Acoustic Fields," *J. of Acoust. Soc. Am.*, Vol. 32, No. 10, pp. 1243~1250.
- (7) Nguyen, N. T. and White, R. M., 1999, "Design and Optimization of an Ultrasonic Flexural Wave Micropump Using Numerical Simulation," *Sensors and Actuators*, Vol. 77, pp. 229~236.
- (8) Gould, R. K., 1966, "Heat Transfer across a Solid-liquid Interface in the Presence of Acoustic Streaming," *J. of Acoust. Soc. Am.*, Vol. 40, No. 1, pp. 219~225.
- (9) Gopinath, A. and Mills, F., 1993, "Convective Heat Transfer From a Sphere Due to Acoustic Streaming," *J. of Heat Transfer*, Vol. 115, pp. 332~341.
- (10) Gopinath, A. and Mills, F., 1994 "Convective Heat Transfer Due to Acoustic Streaming Across the Ends of Kundt Tube," *Journal of Heat Transfer*, Vol. 116, pp. 47~53.
- (11) Uhlenwinkel, V., R. Meng, K. Bauckhage, P., Schreckenber, and Andersen, O., 1994 "Heat Transfer to Cylindrical Bodies and Small Particles in an Ultrasonic Standing-wave Fields of Melt Atomizer," *Multiphase-flow and Heat Transfer in Materials Processing ASME, FED-Vol.201/HTD-Vol. 297*, pp. 19~24.
- (12) Vainshtein, P., Fichman, M. and Cutfinger, C., 1995, "Acoustic Enhancement of Heat Transfer Between Two Parallel Plates," *Int. J. Heat & Mass Transfer*, Vol. 38, No. 10, pp.

1893~1899.

(13) Chen, Z. D., Taylor, M. P. and Chen, J. J. 1998, "Heat Transfer on a Surface Affected by an Air/Water Interface Undergoing Wave Motion," The Minerals, Metals & Materials Society, pp. 429~435.

(14) Uchida, Toyokazu, Suzuki, Takayuki, and Shiokawa, Showko, "Investigation of Acoustic Streaming Excited by Surface Acoustic Waves," 1995 IEEE Ultrasonics Symposium, pp. 1081~

1084.

(15) Moroney, R. M., White, R. M, and Howe, R. T.. "Ultrasonically Induced Microtransport," Proceedings of 1991 IEEE Micro Electro Mechanical Systems, pp. 277~282.

(16) Sashida, T, 1993, An Introduction to Ultrasonic Motors, Clarendon Press, Oxford.

(17) Kays, W. M. and Crawford, M. E., 1993 Convective Heat and Mass Transfer, McGraw-Hill, New York.